

Article

Factors Affecting Droplet Loss behind Canopies with Air-Assisted Sprayers Used for Fruit Trees

Shijie Jiang , Wenwei Li, Shenghui Yang , Yongjun Zheng *, Yu Tan and Jiawei Xu

College of Engineering, China Agricultural University, Beijing 100083, China

* Correspondence: zyj@cau.edu.cn

Abstract: Air-assisted sprayers are widely employed in orchards, but inappropriate spray parameters can lead to large droplet losses, pesticide waste, and environmental pollution. To investigate the factors affecting the droplet loss of an air-assisted sprayer behind canopies, a two-factor, five-level full experiment was conducted in an actual orchard, where the two factors were the power gradient and foliage area volume density (FAVD). In addition, the location of the sampling point was also considered in the data analysis, including horizontal distance, forward distance, and height. The results show that all factors significantly affected droplet coverage (p -value < 0.01). The droplet coverage showed an increase and then a decrease with an increasing power gradient, and the maximum coverage was measured at power gradient P3 (forward speed: 0.49 m/s, spray pressure: 0.30 MPa, and spray flow rate: 7.13 L/min) or P4 (forward speed: 0.58 m/s, spray pressure: 0.35 MPa, and spray flow rate: 8.44 L/min). The effect of FAVD on droplet coverage had obvious regularity, and this regularity did not change with the power gradient. At different positions behind canopies, the droplet coverage had great differences. The droplet coverage gradually decreases with increasing horizontal distance and height, while increasing with forward distance. This study provides a reference for the air-assisted sprayers to reduce droplet loss, and data support for subsequent research on precision spraying based on FAVD.

Keywords: air-assisted sprayer; behind canopies; droplet loss; foliage area volume density (FAVD); environmental pollution; orchard



Citation: Jiang, S.; Li, W.; Yang, S.; Zheng, Y.; Tan, Y.; Xu, J. Factors Affecting Droplet Loss behind Canopies with Air-Assisted Sprayers Used for Fruit Trees. *Agronomy* **2023**, *13*, 375. <https://doi.org/10.3390/agronomy13020375>

Academic Editor: Yanbo Huang

Received: 25 December 2022

Revised: 25 January 2023

Accepted: 25 January 2023

Published: 27 January 2023



Copyright: © 2023 by the authors. Licensee MDPI, Basel, Switzerland. This article is an open access article distributed under the terms and conditions of the Creative Commons Attribution (CC BY) license (<https://creativecommons.org/licenses/by/4.0/>).

1. Introduction

Air-assisted sprayers are widely employed in orchards to improve spray efficiency [1,2]. Droplets rely on the air-assisted sprayer's fan to obtain a greater initial velocity, while the airflow generated by the fan enables leaves to turn over. The flow enhances the droplet deposition within canopies. However, if the operating parameters are not properly set, droplets will be carried away by the airflow, resulting in droplet loss, which mainly contains the deposition loss to the ground and the diffusion loss to the air [3–5]. Off-target losses lead to the pollution of the orchard environment. Especially, the loss behind canopies facilitates pesticide residues in neighboring crops and soils [6–8], which is the main form of pesticide pollution to the environment [9,10].

Current research on anti-drift air-assisted sprayers focuses on developing anti-drift technologies to enhance droplet deposition in canopies to reduce drift [11–13]. Computational Fluid Dynamics (CFD) simulation is a common method to study droplet loss and drift. Pascuzzi et al. performed a numerical simulation to analyze the drift patterns of the droplets with different diameters influenced by airflow directions [14]. Hong et al. evaluated the droplet deposition and drift loss from an air-assisted sprayer in the form of CFD simulation [15]. Duga et al. developed a CFD model for drift from an air-assisted sprayer, and analyzed the effect of nozzle position, number of nozzles, and fan speed on droplet drift based on this model [16]. Although CFD simulations predict the deposition and drift of droplets, there are differences between the simulated and actual environments.

The simulation results can only serve as a reference and still need to be verified by actual operation. In terms of anti-drift technology and mechanism improvement, conical airflow anti-drift devices [17,18], anti-drift nozzles [19,20], and other mechanisms were designed [21]. Rathnayake et al. evaluated the downwind drift characteristics of air-assisted sprayers in apple orchards and found that the drift distance of droplets in the downwind direction would exceed 183 m [22]. In addition, applicable methods for the evaluation of pesticide droplet drift or loss were developed [23,24]. These studies provided useful implications for the improvement of air-assisted spraying technology and the selection of application parameters. The canopy characteristics had a great influence on droplet drift in actual operations [25–27]. However, these characteristics were not considered in the studies. Therefore, the factors affecting droplet drift or loss in practice are not well-understood, and further research is needed.

In this paper, an experiment was conducted in an orchard to investigate the factors influencing the droplet loss of air-assisted sprayers behind canopies. The purpose is to clarify the effects of different factors on droplet loss behind canopies and quantify each factor's impact. This study provides a reference for air-assisted sprayers to reduce droplet loss in orchard spraying.

2. Materials and Methods

2.1. Air-Assisted Sprayer

A tower-type air-assisted sprayer, G6S, was selected (Figure 1A), which was produced by Shandong Guohaha Agricultural Machinery Co., Ltd. (Linyi, China). The main technical parameters are: the overall dimensions of the G6S air-assisted sprayer are $2500 \times 1050 \times 1500$ mm, the maximum capacity of the tank is 350 L, the maximum spray pressure is 2.0 MPa, the pump is a three-cylinder plunger pump, and the maximum flow rate of the pump is 48 L/min. The nozzle is a small bee nozzle (Shandong Guohaha Agricultural Machinery Co., Ltd., Linyi, China), which is a two-way nozzle that combines a fan-shaped and a conical nozzle (Figure 1B). Spraying was performed with the fan-shaped nozzle during the experiment, and the spray angle of the fan-shaped nozzle is 65° . All 18 nozzles are symmetrically distributed on both sides of the tower. The forward speed, fan speed, and pressure of the sprayer are directly controlled by the throttle, which is commonly used for air-assisted sprayers in orchards in China at present.

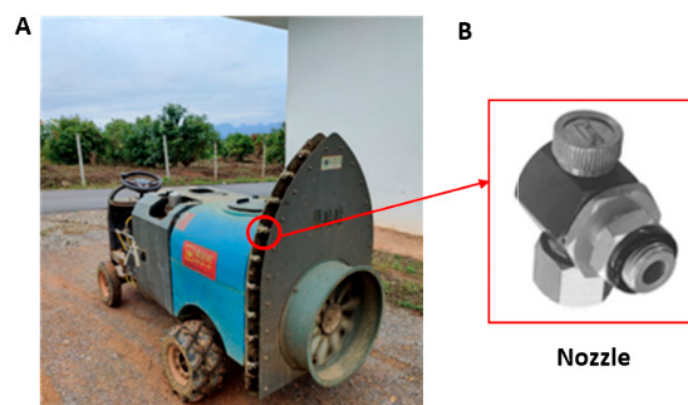


Figure 1. G6S tower air-assisted sprayer.

2.2. Experimental Scheme

The experiment was conducted from 8 to 25 April 2020 in Tianyang District, Baise City, Guangxi Zhuang Autonomous Region, China. The fruit tree is mango with large canopies. Planting parameters such as row spacing, plant spacing, and plant height were determined in the experimental area by randomly measuring 30 times with a tape measure. Row spacing, plant spacing, and plant height were on average 4.5, 3.5, and 4.5 m, respectively.

A two-factor, five-level full experiment was conducted. The two factors were the power gradient and the foliage area volume density (FAVD) of the fruit tree canopy.

FAVD is the sum of the leaf area per unit volume at a certain height (m^2/m^3). The FAVD at different positions of the canopy is different. Therefore, the average FAVD at different positions of fruit tree canopies was used to represent the FAVD of the whole tree. Five fruit trees were randomly selected as the five levels of the FAVD, labeled Tree1, Tree2, Tree3, Tree4, and Tree5. The measurement method is described as follows:

- (a) A $50 \times 50 \times 50$ cm cubical frame was selected to randomly frame the canopy 5 times.
- (b) The number of leaves in the frame was counted, and the average value was calculated.
- (c) The average area of individual leaves of fruit trees was calculated using the following image processing method [28]:
 - ◆ Pre-processing the acquired image.
 - ◆ Segmenting the labeled images to obtain target images.
 - ◆ Calculating the actual area of the leaf by the reference method.
- (d) The FAVD of each fruit tree was calculated based on Equation (1):

$$FAVD = \frac{N \times S_{leaf}}{V} \quad (1)$$

where S_{leaf} is the area of the leaf, N is the average number of leaves in the cubical frame, and V is the volume of the cubical frame.

Spray experiments were conducted at five power gradient levels. These levels were the five positions of the air-assisted sprayer throttle, marked P1, P2, P3, P4, and P5. The five power gradients were calibrated before the start of the experiment. Per power gradient, the average forward speed was determined by recording the time to cross a distance of 30 m, 5 times. The time of each case was recorded, and then the ratio of distance to time was calculated to obtain the average speed. The fan speed was measured five times by a UNI-T UT370 photoelectric tachometer (UNI-Trend Technology (China) Co., Ltd., Dongguan, China) for each power gradient and then averaged. The airflow rate at each nozzle outlet was measured by a Testo 405i thermal wireless anemometer (Testo AG, Titisee-Neustadt, Germany), so there were 18 anemometers in total. Per power gradient, data were continuously collected for 30 s (about 15 data points). The average of these 15 data points was selected as the outlet airflow rate of the corresponding nozzle. The Testo 405i thermal wireless anemometer was connected to an android phone via Bluetooth to save the data in real time.

Spray pressure and spray flow rate can be calculated according to Equations (2) and (3):

$$P_{pressure} = \frac{V_{test}}{V_{max}} \times P_{max} \quad (2)$$

$$F_{flow} = \frac{V_{test}}{V_{max}} \times F_{max} \quad (3)$$

where $P_{pressure}$ is the spray pressure, V_{test} is the forward speed calibration value, V_{max} is the maximum forward speed, P_{max} is the maximum spray pressure, F_{flow} is the spray flow rate, and F_{max} is the maximum spray flow rate.

The experimental scheme is shown in Figure 2. First, $3 \times 3 \times 3$ sampling points (27 sampling points) were arranged behind the canopies of 5 fruit trees and divided into 3 layers: top, middle, and bottom. Second, the sampling points of each layer were labeled in the order of 1–9. To express each location more clearly, measurement locations were defined. For example, the location of sampling point 1 at the top layer was described as ‘1 top’, and that at the bottom layer was defined as ‘1 bottom’. The horizontal distance from the central line of the sprayer to the tree center was 1.8 m. The horizontal distance from the center of the tree to the first sampling point was 1.8 m. In each layer, the distance between sampling points was 1.2 m, the distance between each layer was 0.8 m, and the

distance from the bottom layer to the ground was 0.8 m. Therefore, the sampling distances from the center of the tree were 1.8, 3.0, and 4.2 m, respectively. The heights were 0.8, 1.6, and 2.4 m, respectively. The distances along the trees were 0, 1.2, and 2.4 m, respectively. Water-sensitive paper (WSP) (76×26 mm) was used to collect droplets, which was fixed at each sampling point with paper clips. For safety reasons and the impact on fruit trees, water was chosen as the solution during the experiment.

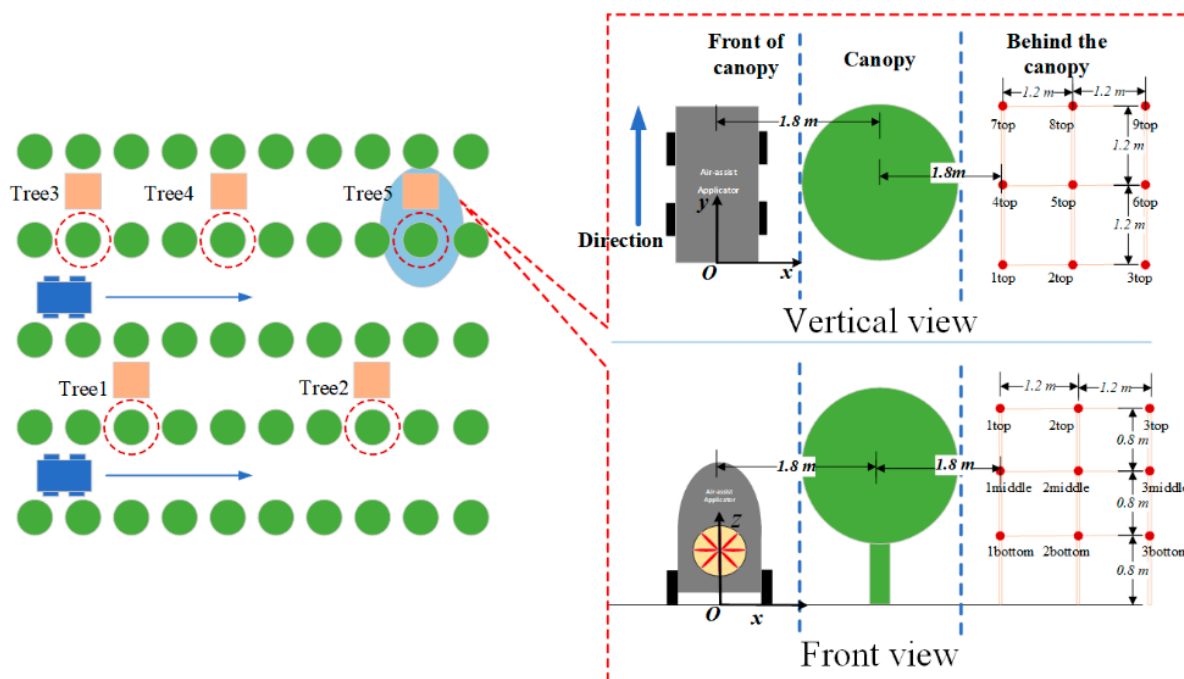


Figure 2. Schematic of the experimental scheme.

Before each experiment, the WSPs were arranged on the sampling points. Then, the air-assisted sprayer was started, the power gradient was varied, the nozzle was turned on, and the sprayer was steadily run to pass by the test fruit trees at a uniform speed along the centerline between the rows. After traveling to a distance of 20 m from the test fruit trees, the sprayer was turned off. After drying, the WSPs were collected and scanned. The above experimental process was repeated in the order of Tree1 to Tree5 and power gradient P1 to P5, with a minimum interval of 30 min between each experimental group. In total, 675 samples were thus collected.

To facilitate the analysis of each sampling point's location, a three-dimensional coordinate system (O-XYZ) was constructed. The intersection of the plane containing the sampling points 1, 2, and 3 was taken as well as the sprayer central axis and the ground as the coordinate origin O. The direction vertical to the forward orientation was the X-positive direction, the direction of forward orientation was the Y-positive direction, and the vertical direction upward from the ground was the Z-positive direction.

X represents the horizontal diffusion direction of droplets, which was used for the subsequent analysis of the correlation between droplet coverage and horizontal distance. Y represents the forward diffusion direction of droplets with the sprayer, which was used for the analysis of the correlation between droplet coverage and forward distance. Z represents the vertical diffusion direction of droplets, which was used for the analysis of the correlation between droplet coverage and height.

2.3. Data Analysis Methods

2.3.1. Selection of Dependent Variables

The WSPs collected by the experiment were processed using DepositScan™ software (version 1.2). The parameters used to represent the spray effect commonly include droplet coverage and droplet quantities. The data of the two parameters were read and saved in an Excel file. In this study, the F-test was used to obtain the consistency between the two parameters, and the appropriate parameter was selected as the dependent variable for the subsequent analysis.

As the units of the two parameters were not the same, the values were first normalized separately according to Equation (4) before the analysis:

$$x^* = \frac{x_i - x_{min}}{x_{max} - x_{min}} \quad (4)$$

where x^* is the normalized result, x_i is the original data, x_{min} is the minimum value of the original data, x_{max} is the maximum value of the original data, and i is the ordinal number.

2.3.2. Variables' Significance Based on Analysis of Variance (ANOVA)

Five variables (FAVD, power gradient, horizontal distance (X), forward distance (Y), and height (Z)) were selected as factors during the experiment. The droplet coverage at the sampling site locations was selected as the dependent variable in a multi-way ANOVA, with the magnitude of the p -value indicating the significant factors.

Based on the ANOVA, the effect of these five variables on droplet coverage was separately analyzed and drawn by Origin 2019 for visualization.

For analyzing the effect of the power gradient, the power gradient was utilized as the horizontal axis, and droplet coverage was used as the vertical axis.

For analyzing the effect of FAVD, FAVD was utilized as the horizontal axis, and droplet coverage was used as the vertical axis. The droplet coverage was averaged for all sampling point locations behind canopies. The calculation method is shown in Equation (5):

$$\bar{C} = \frac{\sum_{j=1}^n C_j}{n} \quad (5)$$

where \bar{C} is the average droplet coverage, C_j is the droplet coverage of the j -th sampling point, n is the number of sampling points, $n = 27$, and j is the ordinal number.

For analyzing the droplet coverage difference of the position behind canopies, the three sections in the Y direction ($Y = 0$, $Y = 1.2$ m, and $Y = 2.4$ m) were selected to examine the variation of droplet coverage with horizontal distance and forward distance.

3. Results

3.1. Results of FAVD Calculation and Power Gradient Calibration

FAVD calculation results are shown in Table 1. The power gradient calibration results are shown in Table 2 and Figure 3.

Table 1. FAVD calculation results.

Tree Number	FAVD/(m ² ·m ⁻³)
Tree1	2.72
Tree2	2.32
Tree3	1.50
Tree4	1.92
Tree5	2.22

Table 2. Power gradient calibration results.

Power Gradient	Forward Speed (m·s ⁻¹)	Fan Speed (RPM)	Spray Pressure (MPa)	Spray Flow Rate (L·min ⁻¹)
P1	0.25	9850	0.15	3.63
P2	0.31	10,789	0.19	4.51
P3	0.49	18,820	0.30	7.13
P4	0.58	20,930	0.35	8.44
P5	0.65	22,985	0.39	9.45

Note: All calculated values in the table are average values.

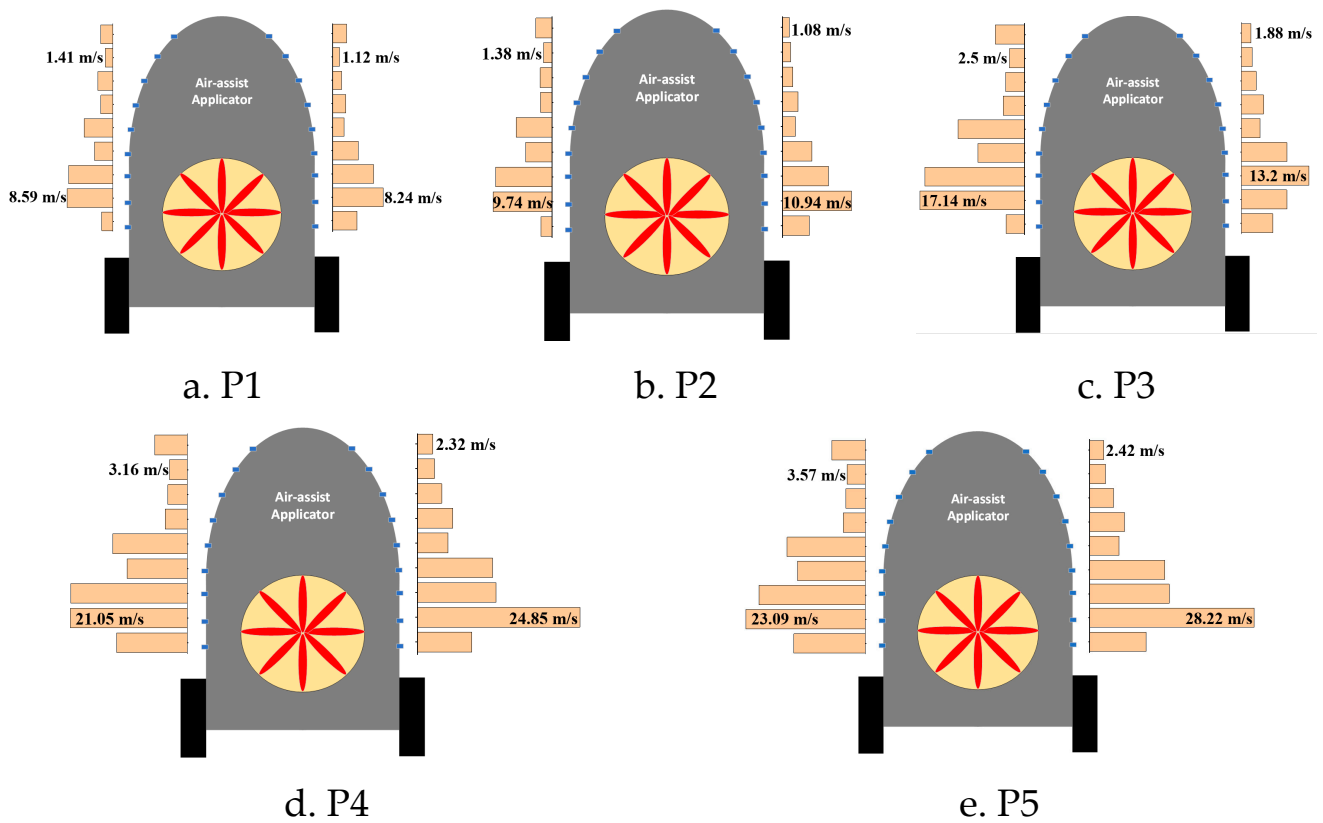


Figure 3. Minimum and maximum airflow rates (m/s) at the nozzle outlets on both sides of the air-assisted sprayer for each power gradient.

3.2. Result of Dependent Variable Selection

An F-test was conducted to observe the consistency between droplet coverage and droplet quantities, and the results are shown in Table 3.

Table 3. F-test results for droplet coverage and droplet quantities.

Tree Number	p-Value
Tree1	0.07
Tree2	0.11
Tree3	0.13
Tree4	0.57
Tree5	0.25

According to the results of the F-test, the p-values of all five trees were greater than 0.05, indicating no significant difference between droplet coverage and droplet quantities.

Therefore, droplet coverage was selected as the dependent variable for subsequent analysis in this study.

3.3. Results of Variables' Significance

The ANOVA results are shown in Table 4.

Table 4. Results of ANOVA on factors influencing droplet coverage behind canopies.

Factor	Spray Variable	F Value	p-Value	Significance
FAVD		7.74	5.56×10^{-3}	**
Power gradient		116.63	$<2.2 \times 10^{-16}$	***
Horizontal distance (X)	Droplet coverage	23.17	1.83×10^{-6}	***
Forward distance (Y)		6.75	9.55×10^{-3}	**
Height (Z)		80.40	$<2.2 \times 10^{-16}$	***

Note: Significance: *** 0.001, ** 0.01.

As can be seen from Table 4:

- (1) For droplet coverage, all five factors were significant. Among them, power gradient, horizontal distance, and height were the most significant, followed by FAVD and forward distance. Although the five factors showed different levels of significance, the *p*-value of each factor was less than 0.01.
- (2) The actual spray needs to combine two factors, FAVD and power gradient, to reduce the droplet coverage behind the canopy. For the actual spray, FAVD is the fruit tree variable and power gradient is the sprayer variable, both of which are decisive for droplet coverage, so it is important to focus on these two variables to reduce the droplet coverage of a non-target (non-canopy).

3.4. Effect of the Power Gradient on Droplet Coverage behind Canopies

The variation of droplet coverage with power gradient is shown in Figure 4.

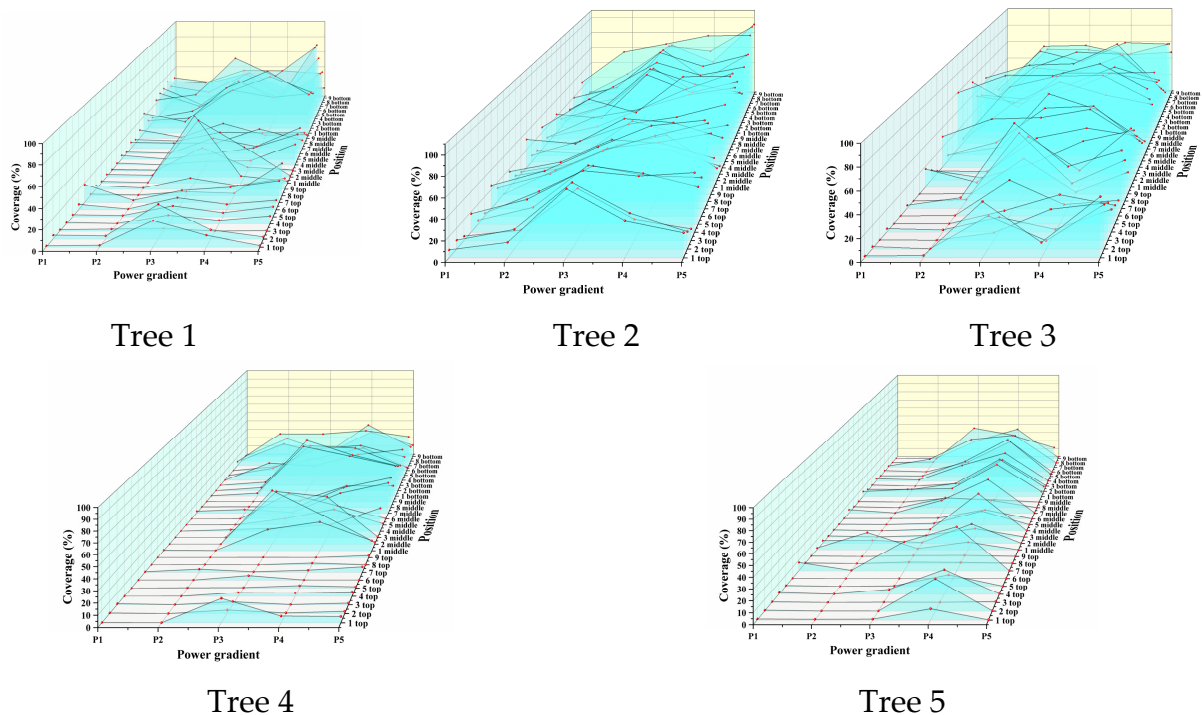


Figure 4. Effect of the power gradient on droplet coverage.

From Figure 4, it can be seen that:

- (1) The power gradients of P1 and P2 may be more suitable for fruit tree spraying. For the five fruit trees, the loss behind the canopy, as expressed as droplet coverage on WSPs, was lower at P1 and P2. According to the authors' previous research [29], the droplet coverage within the canopy could meet the spray requirements when power gradients were P1 and P2. Therefore, P1 or P2 could be preferred for fruit tree spraying to reduce the droplet coverage behind canopies.
- (2) The use of power gradients P3 and P4 could be best avoided when spraying mango trees. The droplet coverage increased first and then decreased with the power gradient. In Figure 4, P3, P4, and P5 reached the highest losses, quantified by droplet coverage. For Tree2 and Tree3, the average droplet coverage at P3 (Tree2: 56.97%, Tree3: 47.22%) was larger than at P5 (Tree2: 54.39%, Tree3: 39.10%), so P3 or P4 resulted in the highest losses, and the actual spraying should pay attention to the serious loss formed by these two power gradients.

3.5. Effect of FAVD on Droplet Coverage behind Canopies

Figure 5 shows the variation of droplet coverage with FAVD. It could be indicated that:

- (1) With the increase of the FAVD, the average coverage of droplets behind canopies under different power gradients showed a decrease, increase, and then a decrease. Overall, the droplet coverage of Tree4 and Tree5 was smaller than that of Tree1, Tree2, and Tree3.
- (2) The power gradient did not change the relationship between FAVD and droplet coverage, but changed the maximum value of average droplet coverage, e.g., P1 maximum value was 12.73% (Tree3), while P5 maximum value was 56.97% (Tree2).
- (3) The effect of FAVD on droplet coverage had obvious regularity, and this regularity did not change with the power gradient. Therefore, in actual spraying, the effect of FAVD on droplet coverage should be considered.

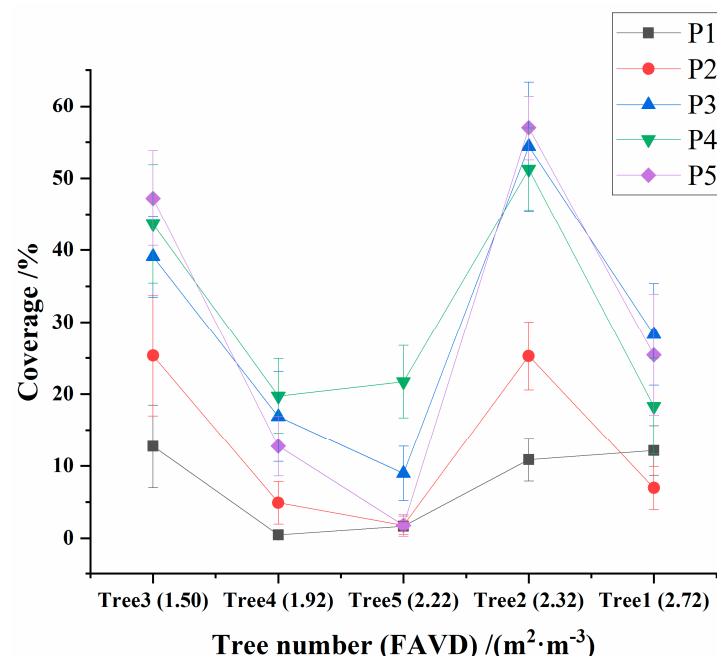


Figure 5. Mean droplet coverage (%) for different FAVD (m^2/m^3) over different power gradients.

3.6. Droplet Coverage Difference of the Position behind Canopies

The variation of droplet coverage in the horizontal distance (X) and height (Z) at $Y = 0$, $Y = 1.2$ m, and $Y = 2.4$ m was separately analyzed. Some of the results are shown in Figures 6–8. All the results are shown in Appendices A–C.

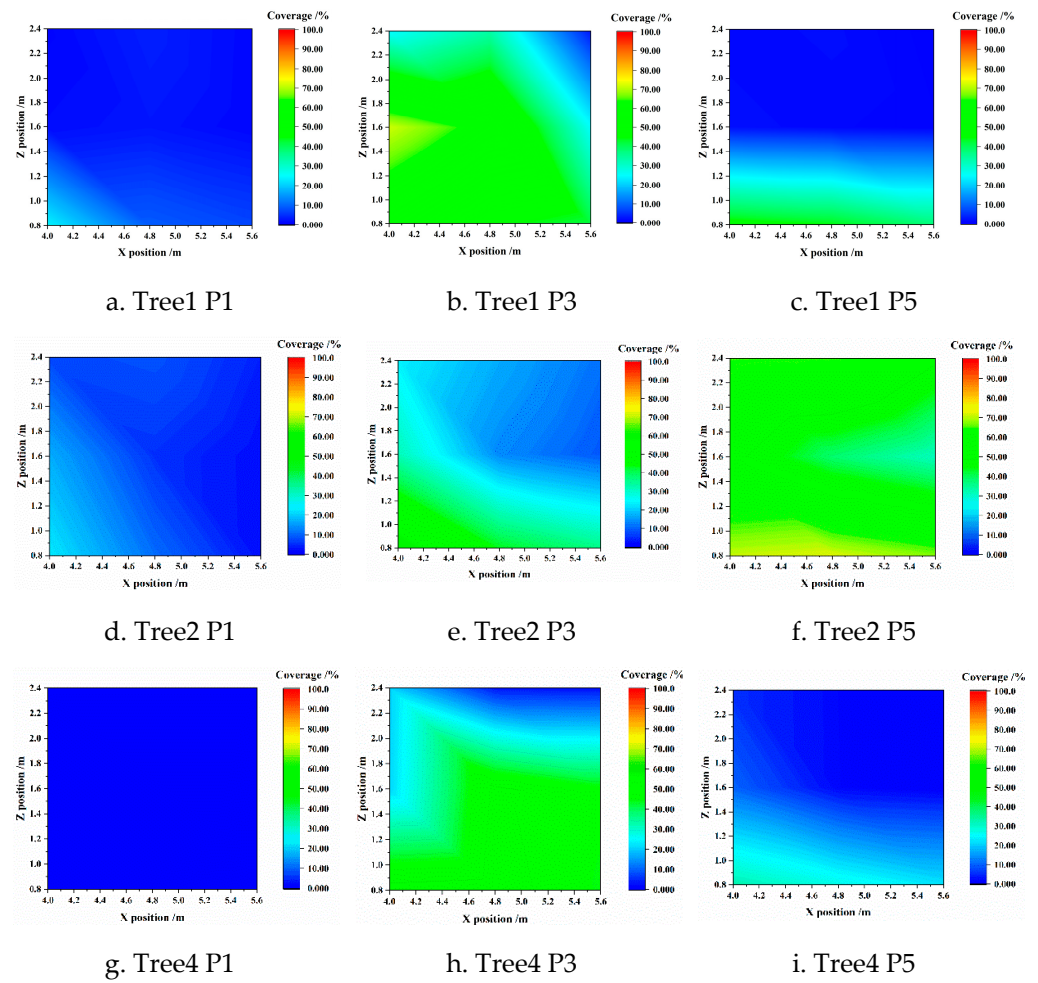


Figure 6. Droplet coverage difference at the position $Y = 0$.

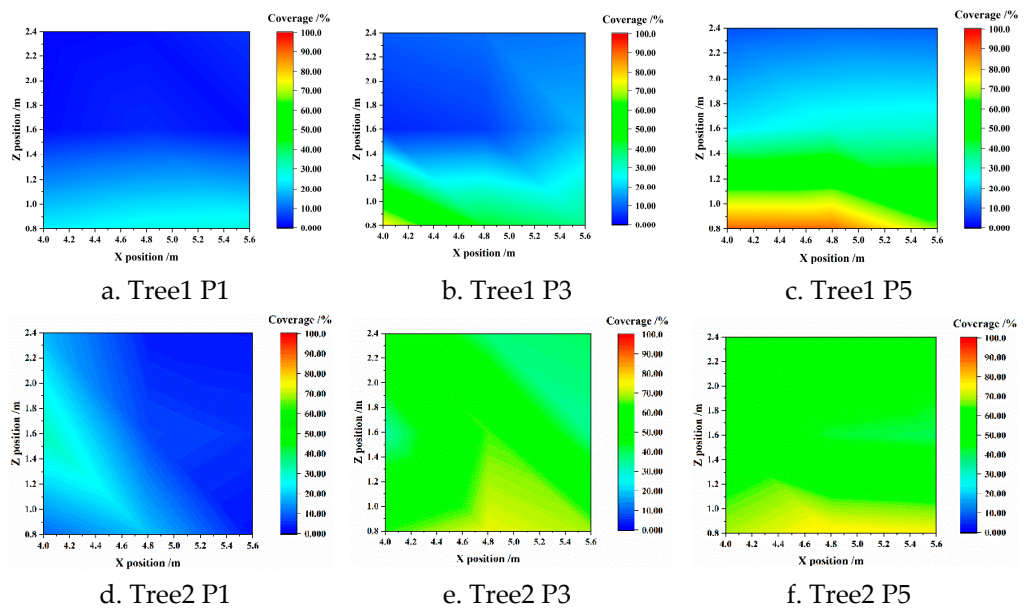


Figure 7. Cont.

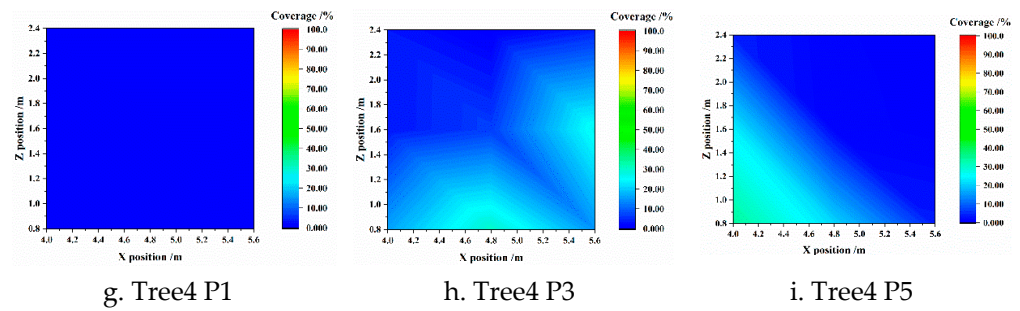


Figure 7. Droplet coverage difference at the position $Y = 1.2$ m.

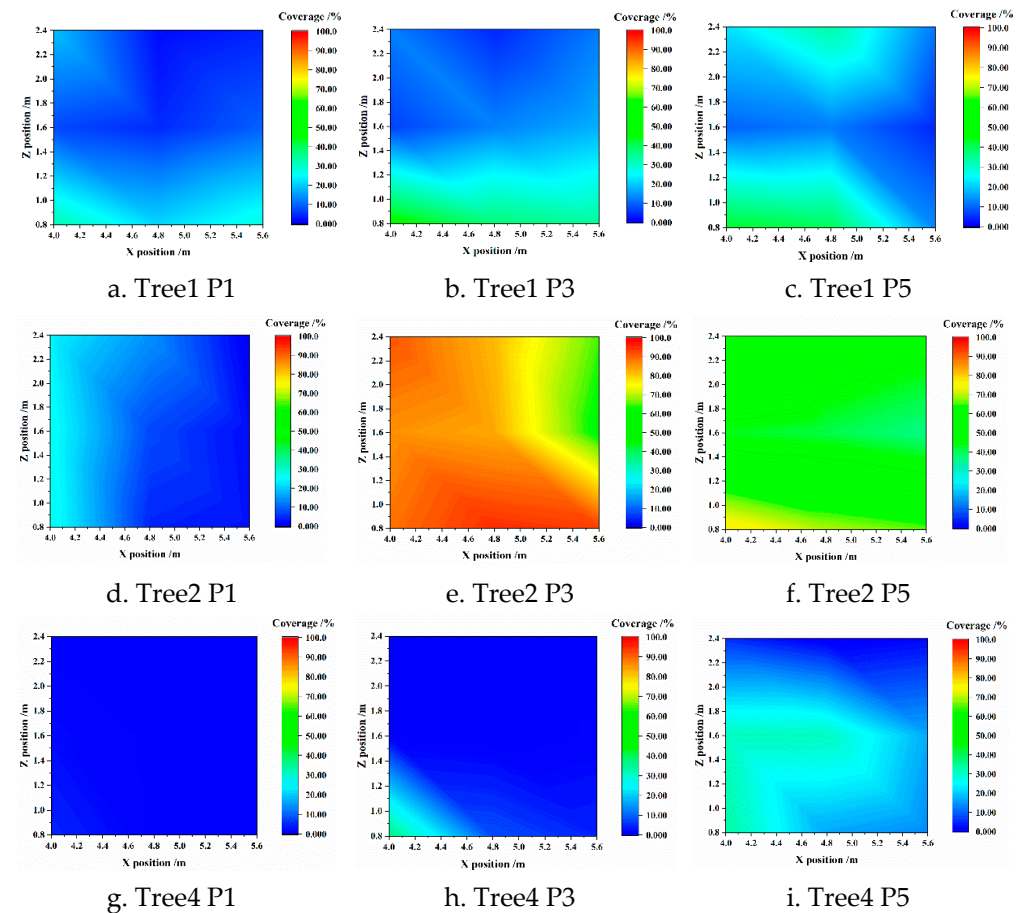


Figure 8. Droplet coverage difference at the position $Y = 2.4$ m.

From Figures 6–8, it can be seen that:

- (1) As the horizontal distance (X) and height (Z) increased, the droplet coverage gradually decreased. During actual spraying, the spray parameters can be appropriately adjusted to improve the droplet coverage of the target and reduce the droplet loss.
- (2) The droplet coverage gradually increased in the Y direction (forward direction). When the FAVD and power gradient were constant, the droplet coverage gradually increased along the Y direction. Although the trends under some conditions were different (such as Tree4 under the P3 power gradient), it did not affect the overall regularity. This may be due to experimental errors caused by environmental factors.
- (3) The possible reasons for the increase of droplet coverage along the Y direction were: the forward speed of the sprayer in the Y direction makes the droplets have an initial velocity, and the droplet coverage in the current section was formed by the

superposition of the current droplets and the previous droplets. Thus, the droplet coverage gradually increased along the Y direction.

- (4) For different power gradients, the variation regularity of droplet coverage along horizontal distance and height did not change, but the value of droplet coverage changed.

4. Discussion

In this study, to explore the loss of droplets behind canopies during spraying of fruit trees by air-assisted sprayers, a two-factor, five-level full experiment was conducted. The FAVD of fruit trees was tested as a factor. To examine the effect of FAVD on droplet loss, the experiment results showed that the FAVD significantly affected the droplet coverage (Table 4 and Figure 5). The FAVD was rarely involved in other studies on the effects of spraying in orchards. It is usually focused on the influence of spray pressure, airflow rate, and other parameters on droplet loss [10,30–32]. Although Sun et al. considered FAVD when studying the droplet penetration model of fruit trees, they did not clarify the effect of FAVD on droplet loss [33].

The application of air-assisted sprayers in orchards has significantly improved spraying efficiency, but it has also caused many problems, such as excessive spraying, pesticide residues, and environmental pollution. Many studies have proven that the adjustment of the pesticide application rate according to the characteristics of the fruit tree canopy is an effective means to reduce pesticide residues and environmental pollution [34–38]. However, the acquisition of canopy features was generally based on the ‘sensor scanning/acquisition-solving geometric equations-fitting canopy profile’ method [39,40], which simplified the asymmetric and porous structure of the canopy. Canopy characteristics mainly include canopy volume, leaf wall area, FAVD, etc. FAVD is the parameter that best reflects the characteristics of the canopy. Based on this study, studying the detection method of FAVD, and adjusting the spraying parameters based on this, will significantly reduce the droplet loss.

This study provides data support for subsequent research on precision spraying based on FAVD. However, there are still some shortcomings:

- (1) In this paper, only one air-assisted sprayer was used as the experimental equipment, and a variety of sprayers can be used for comparative experiments in the future.
- (2) The G6S air-assisted sprayer uses the throttle (power gradient) to simultaneously adjust parameters such as forward speed, fan speed, spray pressure, and spray flow rate. These parameters cannot be separately adjusted, so experiments with different parameter combinations were not conducted.
- (3) In this paper, mango trees with large canopies were used as the experimental trees. Later, experiments can be carried out on different types of fruit trees to explore the regularity of droplet loss in different types of fruit trees.

5. Conclusions

A two-factor, five-level full experiment was conducted in an actual orchard. The effects of the power gradient and FAVD on droplet coverage behind canopies were analyzed, and the droplet coverage difference behind the canopies was clarified. Based on a detailed analysis of the experimental data, the following conclusions were obtained:

- (1) Droplet coverage and droplet quantities were consistent, and five factors (power gradient, FAVD, horizontal distance (X), Forward distance (Y), and height (Z)) were significantly affected by droplet coverage behind the canopies (p -value < 0.01).
- (2) In this study, power gradients P1 (forward speed: 0.25 m/s, spray pressure: 0.15 MPa, and spray flow rate: 3.63 L/min) and P2 (forward speed: 0.31 m/s, spray pressure: 0.19 MPa, and spray flow rate: 4.51 L/min) resulted in the lowest losses behind the canopy, as quantified by droplet coverage on WSPs. Based on the results found in this study, the use of power gradient P3 (forward speed: 0.49 m/s, spray pressure: 0.30 MPa, and spray flow rate: 7.13 L/min) or P4 (forward speed: 0.58 m/s, spray pressure: 0.35 MPa, and spray flow rate: 8.44 L/min) should be avoided.

- (3) The effect of FAVD on droplet coverage had obvious regularity. With the increase of FAVD, droplet coverage first decreased, then increased, and finally, decreased again. This regularity did not change with the power gradient. At different positions behind canopies, the droplet coverage considerably varied. As the horizontal distance (X) and height (Z) increased, the droplet coverage gradually decreased. However, the droplet coverage gradually increased in the Y direction (forward direction).

This study revealed the loss regularity of droplets behind the fruit tree canopy, which can provide reference for the selection of operation parameters. The effect of FAVD on droplet loss was clarified, and data support was provided for the subsequent research on variable spraying based on FAVD.

Author Contributions: S.J., data curation, tests, and writing—original draft; W.L., visualization and tests; S.Y., methodology and writing—review and editing; Y.Z., supervision, methodology, and resources; Y.T., methodology and resources; J.X., tests. All authors have read and agreed to the published version of the manuscript.

Funding: This study was supported and funded by the National Natural Science Foundation of China (NSFC) (32171901), and the YANTAI Locality and University Cooperation Development Project (2021XDRHXMP29).

Institutional Review Board Statement: Not applicable.

Informed Consent Statement: Not applicable.

Data Availability Statement: Not applicable.

Conflicts of Interest: The authors declare no conflict of interest.

Appendix A

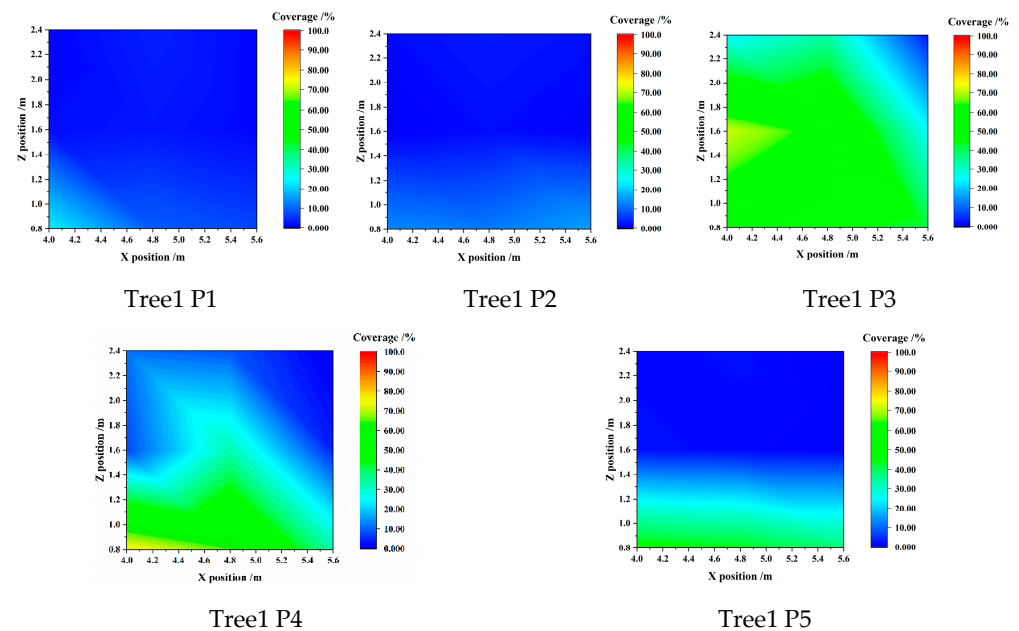


Figure A1. Cont.

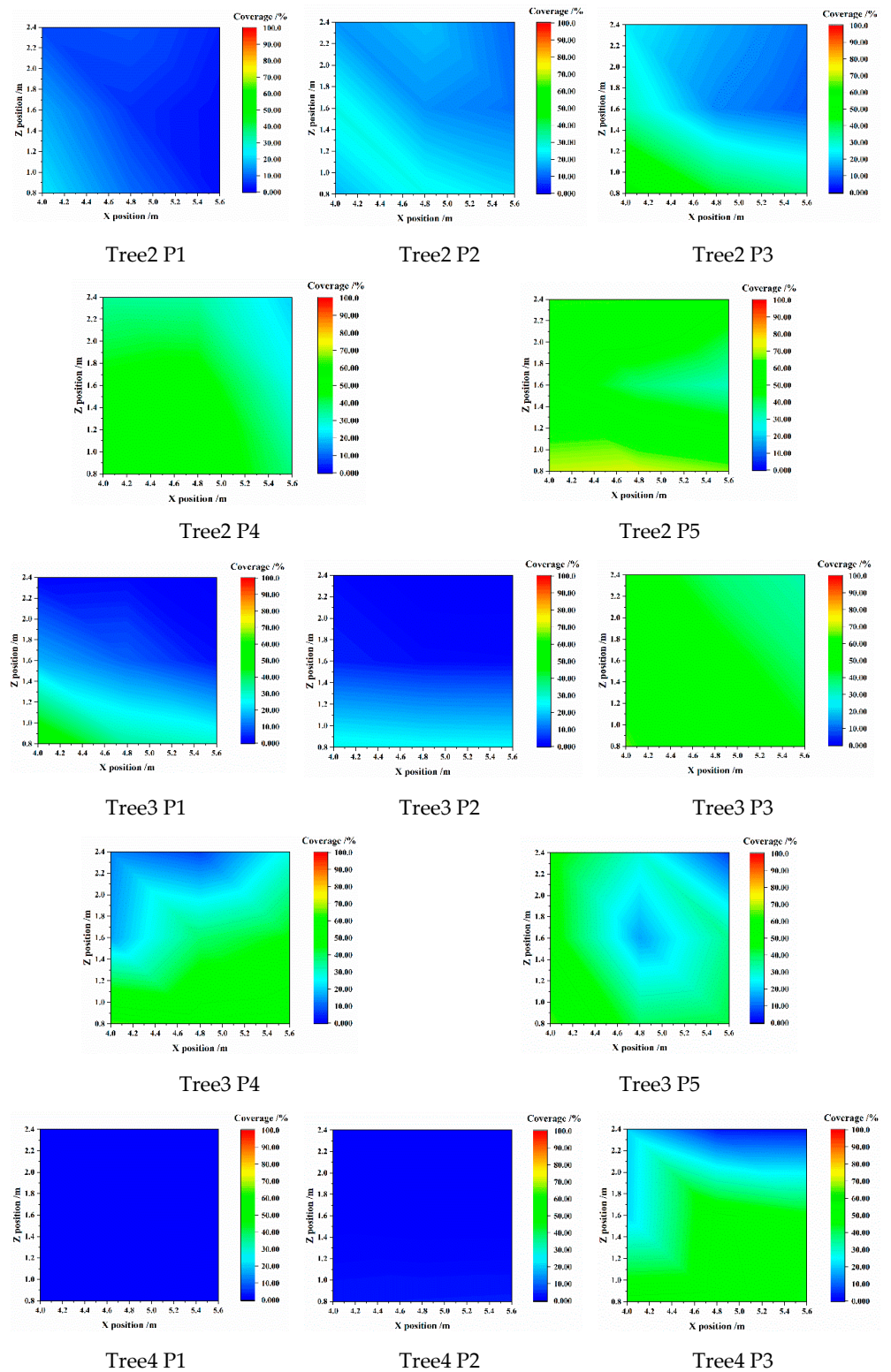


Figure A1. Cont.

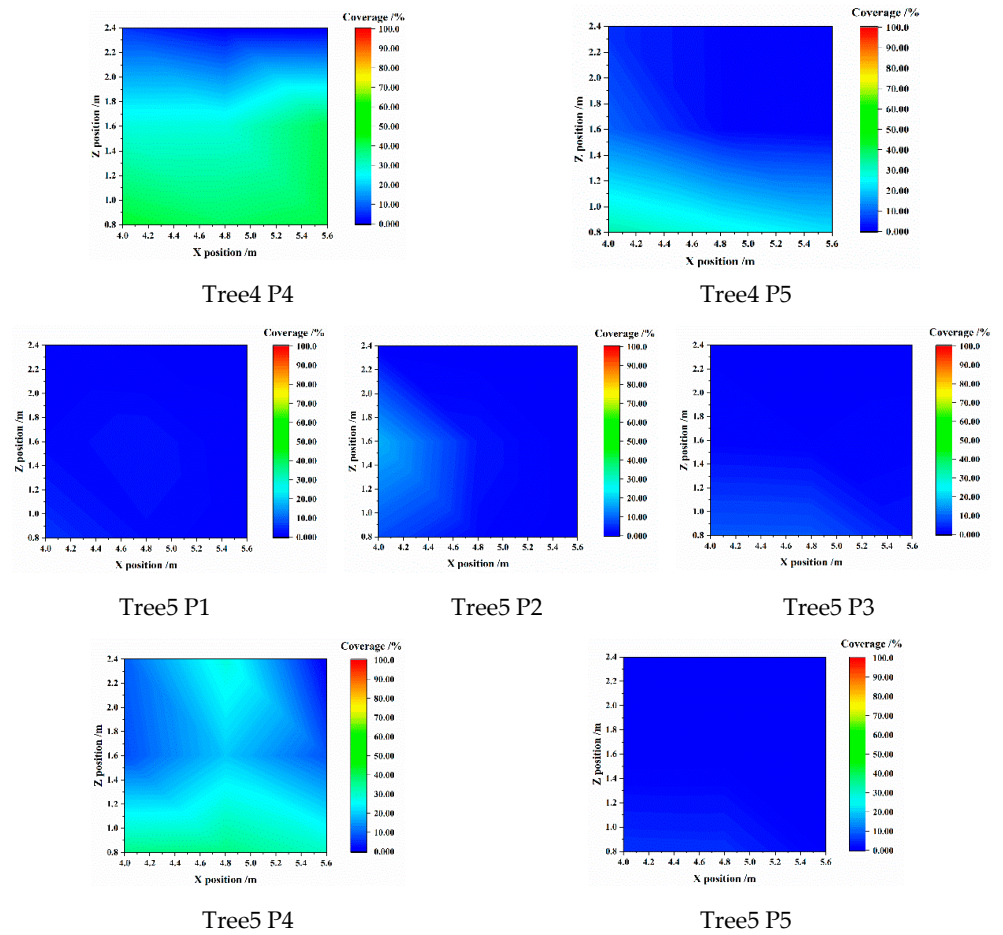


Figure A1. Droplet Coverage Difference at the Position Y = 0.

Appendix B

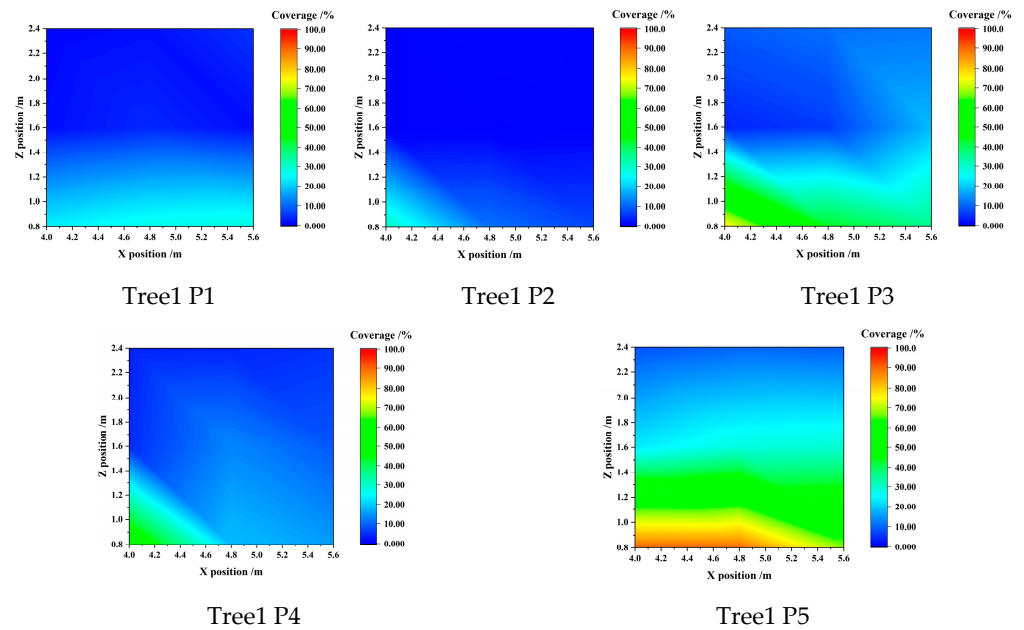


Figure A2. Cont.

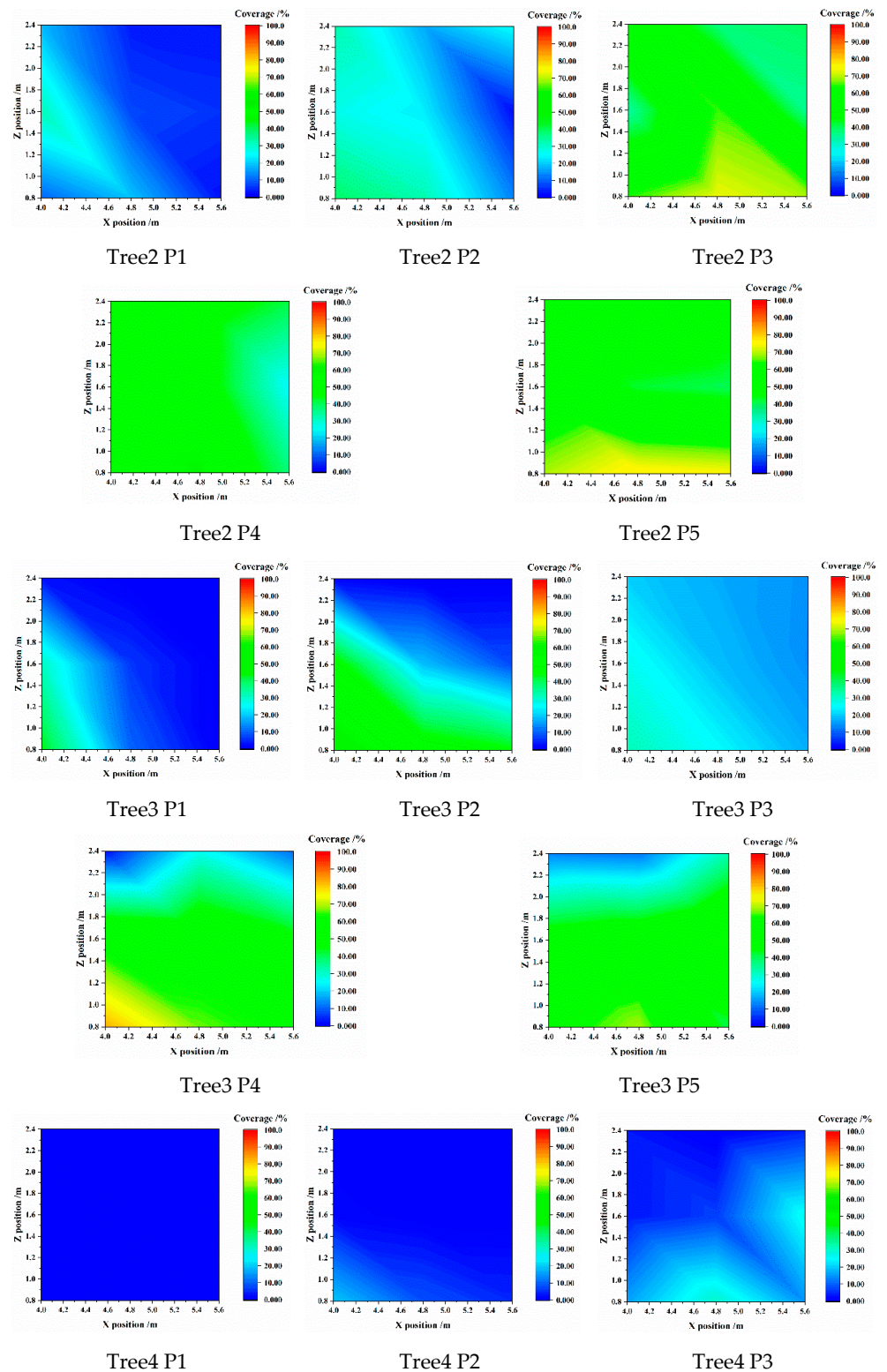


Figure A2. Cont.

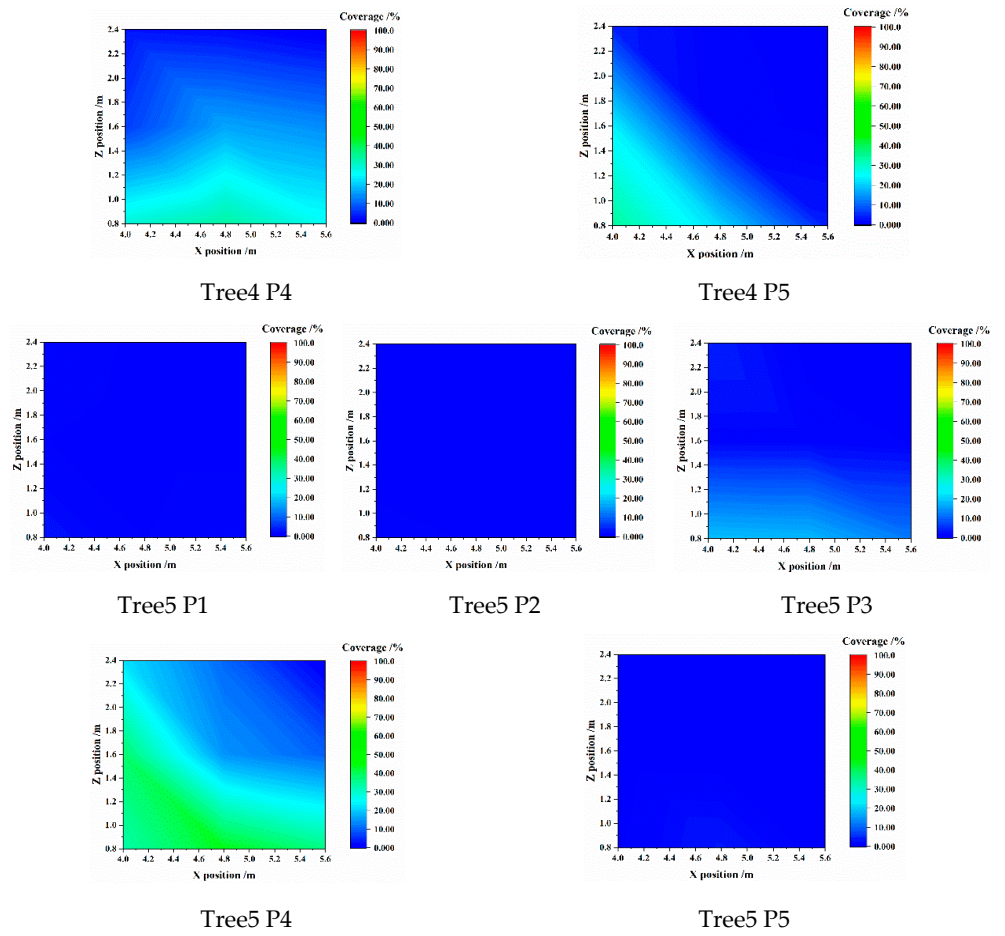


Figure A2. Droplet Coverage Difference at the Position Y = 1.2 m.

Appendix C

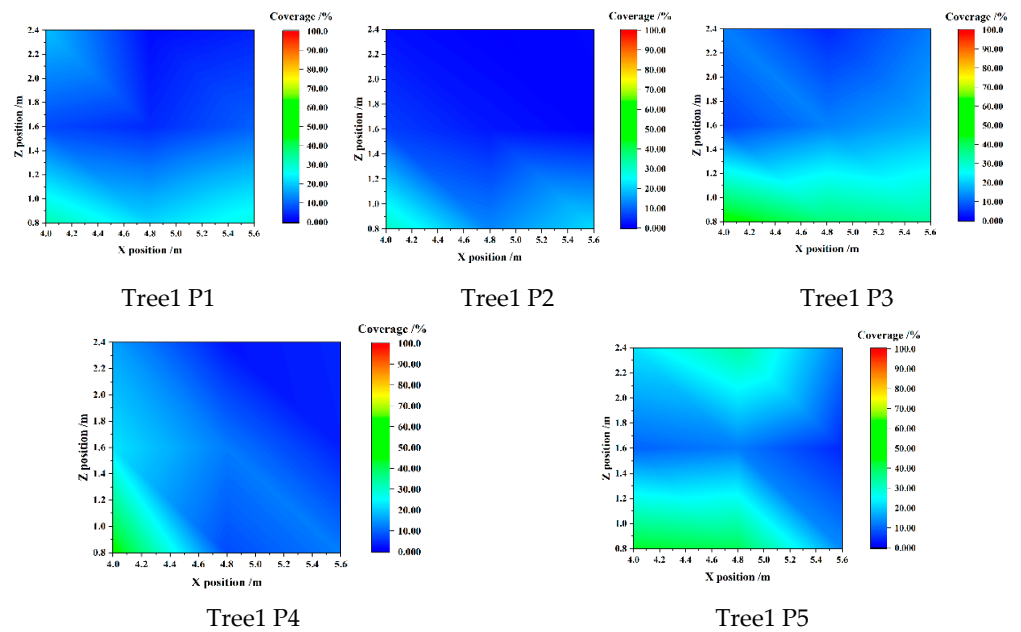


Figure A3. Cont.

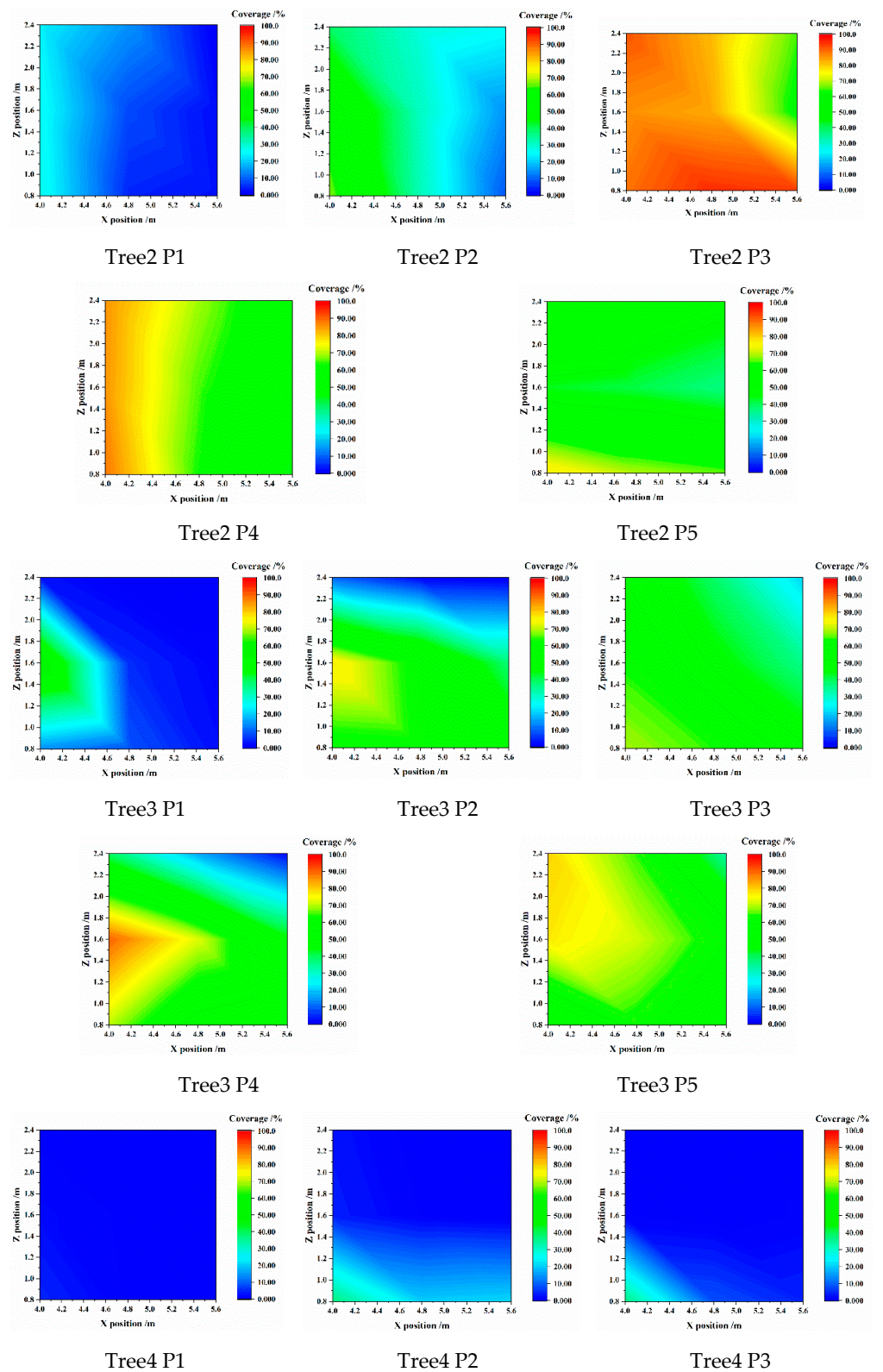


Figure A3. Cont.

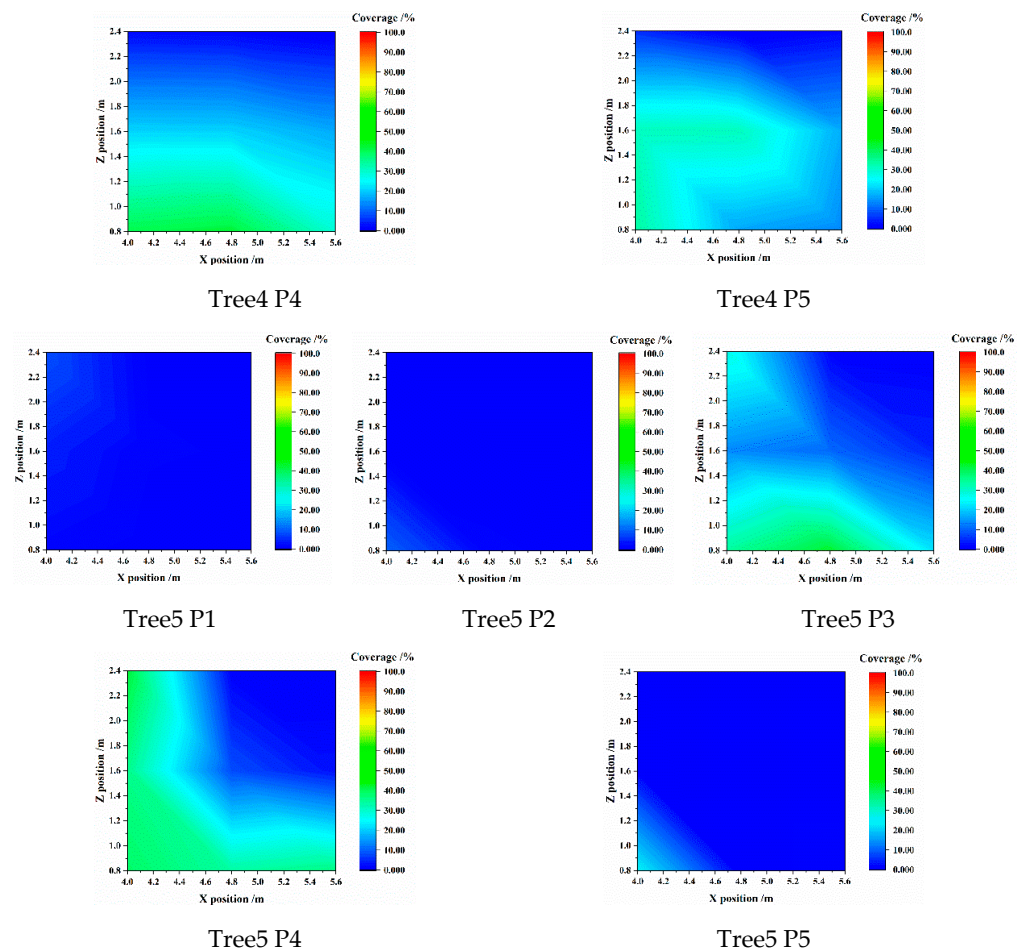


Figure A3. Droplet Coverage Difference at the Position Y = 2.4 m.

References

- Zheng, Y.; Chen, B.; Lv, H.; Kang, F.; Jiang, S. Research progress of orchard plant protection mechanization technology and equipment in China. *Trans. CSAE* **2020**, *36*, 110–124.
- Zheng, Y.; Jiang, S.; Chen, B.; Lv, H.; Wan, C.; Kang, F. Review on technology and equipment of mechanization in hilly orchard. *Trans. Chin. Soc. Agric. Mach.* **2020**, *51*, 1–20.
- Wang, X. Study on Spray Drift and Anti-Drift Method. Ph.D. Thesis, China Agricultural University, Beijing, China, 2017.
- Liu, X.; Yuan, L.; Shi, X.; Du, Y.; Yang, D.; Yuan, H.; Yan, X. Research progress on spray drift of droplets of plant protection machinery. *Chin. J. Pestic. Sci.* **2022**, *24*, 232–247.
- Gil, Y.; Sinfort, C. Emission of pesticides to the air during sprayer application: A bibliographic review. *Atmos. Environ.* **2005**, *39*, 5183–5193. [[CrossRef](#)]
- Zhang, H.; Zheng, J.; Zhou, H.; DORR, G. Droplet Deposition Distribution and Off-target Drift during Pesticide Spraying Operation. *Trans. Chin. Soc. Agric. Mach.* **2017**, *48*, 114–122.
- Soheilifard, F.; Marzban, A.; Raini, M.G.; Taki, M.; van Zelm, R. Chemical footprint of pesticides used in citrus orchards based on canopy deposition and off-target losses. *Sci. Total Environ.* **2020**, *732*, 139118. [[CrossRef](#)] [[PubMed](#)]
- Salcedo, R.; Vallet, A.; Granell, R.; Garcerá, C.; Moltó, E.; Chueca, P. Eulerian–Lagrangian model of the behavior of droplets produced by an air-assisted sprayer in a citrus orchard. *Biosyst. Eng.* **2017**, *154*, 76–91. [[CrossRef](#)]
- Arvidsson, T.; Bergström, L.; Kreuger, J. Spray drift as influenced by meteorological and technical factors. *Pest Manag. Sci.* **2011**, *67*, 586–598. [[CrossRef](#)]
- Grella, M.; Gallart, M.; Marucco, P.; Balsari, P.; Gil, E. Ground Deposition and Airborne Spray Drift Assessment in Vineyard and Orchard: The Influence of Environmental Variables and Sprayer Settings. *Sustainability* **2017**, *9*, 728. [[CrossRef](#)]

11. Fornasiero, D.; Mori, N.; Tirello, P.; Pozzebon, A.; Duso, C.; Tescari, E.; Bradascio, R.; Otto, S. Effect of spray drift reduction techniques on pests and predatory mites in orchards and vineyards. *Crop Prot.* **2017**, *98*, 283–292. [[CrossRef](#)]
12. Ru, Y.; Chen, X.; Liu, B.; Wang, S.; Lin, M. Optimized design and performance test of axial flow orchard sprayer air delivery system. *Trans. Chin. Soc. Agric. Mach.* **2022**, *53*, 147–157.
13. Miranda-Fuentes, A.; Rodríguez-Lizana, A.; Cuenca, A.; González-Sánchez, E.; Blanco-Roldán, G.; Gil-Ribes, J. Improving plant protection product applications in traditional and intensive olive orchards through the development of new prototype air-assisted sprayers. *Crop Prot.* **2017**, *94*, 44–58. [[CrossRef](#)]
14. Pascuzzi, S.; Bulgakov, V.; Santoro, F.; Anifantis, A.S.; Ivanovs, S.; Holovach, I. A Study on the Drift of Spray Droplets Dipped in Airflows with Different Directions. *Sustainability* **2020**, *12*, 4644. [[CrossRef](#)]
15. Hong, S.-W.; Zhao, L.; Zhu, H. CFD simulation of pesticide spray from air-assisted sprayers in an apple orchard: Tree deposition and off-target losses. *Atmos. Environ.* **2018**, *175*, 109–119. [[CrossRef](#)]
16. Duga, A.T.; Delele, M.A.; Ruysen, K.; Dekeyser, D.; Nuyttens, D.; Bylemans, D.; Nicolai, B.M.; Verboven, P. Development and validation of a 3D CFD model of drift and its application to air-assisted orchard sprayers. *Biosyst. Eng.* **2017**, *154*, 62–75. [[CrossRef](#)]
17. Liu, C.; Hu, J.; Li, Y.; Zhao, S.; Zhang, W.; Li, Q. Optimization of the inner flow channel of conical wind field anti-drift spray device and anti-drift characteristics. *Trans. CSAE* **2021**, *37*, 11–20.
18. Hu, J.; Liu, C.; Chu, X.; Li, Y.; Sun, S.; Zhang, W. Droplet deposition characteristics of conical wind field anti-drift device. *Trans. Chin. Soc. Agric. Mach.* **2020**, *51*, 142–149, 174.
19. Sun, D.; Zhan, X.; Liu, W.; Xue, X.; Xie, J.; Li, Z.; Song, S.; Wang, W. Compensation of spray angle to droplet drift under crosswind. *Trans. CSAE* **2021**, *37*, 80–89.
20. Grella, M.; Miranda-Fuentes, A.; Marucco, P.; Balsari, P.; Gioelli, F. Development of Drift-Reducing Spouts For Vineyard Pneumatic Sprayers: Measurement of Droplet Size Spectra Generated and Their Classification. *Appl. Sci.* **2020**, *10*, 7826. [[CrossRef](#)]
21. Grella, M.; Miranda-Fuentes, A.; Marucco, P.; Balsari, P. Field assessment of a newly-designed pneumatic spout to contain spray drift in vineyards: Evaluation of canopy distribution and off-target losses. *Pest Manag. Sci.* **2020**, *76*, 4173–4191. [[CrossRef](#)] [[PubMed](#)]
22. Rathnayake, A.P.; Khot, L.R.; Hoheisel, G.A.; Thistle, H.W.; Teske, M.E.; Willett, M.J. Downwind Spray Drift Assessment for Airblast Sprayer Applications in a Modern Apple Orchard System. *Trans. ASABE* **2021**, *64*, 601–613. [[CrossRef](#)]
23. Wang, Z.; He, X.; Li, T.; Huang, M.; Zhang, Y.; Xu, L.; Deng, X. Evaluation method of pesticide droplet drift based on laser imaging. *Trans. CSAE* **2019**, *35*, 73–79.
24. Grella, M.; Marucco, P.; Balsari, P. Toward a new method to classify the airblast sprayers according to their potential drift reduction: Comparison of direct and new indirect measurement methods. *Pest Manag. Sci.* **2019**, *75*, 2219–2235. [[CrossRef](#)]
25. Fessler, L.; Fulcher, A.; Lockwood, D.; Wright, W.; Zhu, H. Advancing Sustainability in Tree Crop Pest Management: Refining Spray Application Rate with a Laser-guided Variable-rate Sprayer in Apple Orchards. *Hortscience* **2020**, *55*, 1522–1530. [[CrossRef](#)]
26. García-Ramos, F.J.; Serreta, A.; Boné, A.; Vidal, M. Applicability of a 3D Laser Scanner for Characterizing the Spray Distribution Pattern of an Air-Assisted Sprayer. *J. Sens.* **2018**, *2018*, 1–7. [[CrossRef](#)]
27. Chen, L.; Wallhead, M.; Reding, M.; Horst, L.; Zhu, H. Control of Insect Pests and Diseases in an Ohio Fruit Farm with a Laser-guided Intelligent Sprayer. *Horttechnology* **2020**, *30*, 168–175. [[CrossRef](#)]
28. Ren, D.; Feng, T.; Li, Y.; Ren, H. Research and implementation of living leaf area measurement based on plant image. *Intell. Comput. Appl.* **2019**, *9*, 173–176.
29. Jiang, S.; Yang, S.; Xu, J.; Li, W.; Zheng, Y.; Liu, X.; Tan, Y. Wind field and droplet coverage characteristics of air-assisted sprayer in mango-tree canopies. *Pest Manag. Sci.* **2022**, *78*, 4892–4904. [[CrossRef](#)]
30. Ding, S.; Xue, X.; Dong, X.; Gu, W.; Zhou, Q. Effects of spraying parameters on droplet deposition performance. *Trans. Chin. Soc. for Agric. Mach.* **2020**, *51*, 308–315.
31. Qiu, W.; Zhao, S.; Ding, W.; Sun, C.; Lu, J.; Li, Y.; Gu, J. Effects of fan speed on spray deposition and drift for targeting air-assisted sprayer in pear orchard. *Int. J. Agric. Biol. Eng.* **2016**, *9*, 53–62.
32. Li, T.; Qi, P.; Wang, Z.; Xu, S.; Huang, Z.; Han, L.; He, X. Evaluation of the Effects of Airflow Distribution Patterns on Deposit Coverage and Spray Penetration in Multi-Unit Air-Assisted Sprayer. *Agronomy* **2022**, *12*, 944. [[CrossRef](#)]
33. Sun, C.; Liu, C. Construction and application of droplet canopy penetration model for air-assisted spraying pattern. *Trans. CSAE* **2019**, *35*, 25–32.
34. Salcedo, R.; Zhu, H.; Zhang, Z.; Wei, Z.; Chen, L.; Ozkan, E.; Falchieri, D. Foliar deposition and coverage on young apple trees with PWM-controlled spray systems. *Comput. Electron. Agric.* **2020**, *178*, 105794. [[CrossRef](#)]
35. Manandhar, A.; Zhu, H.; Ozkan, E.; Shah, A. Techno-economic impacts of using a laser-guided variable-rate spraying system to retrofit conventional constant-rate sprayers. *Precis. Agric.* **2020**, *21*, 1156–1171. [[CrossRef](#)]
36. Cai, J.; Wang, X.; Gao, Y.; Yang, S.; Zhao, C. Design and performance evaluation of a variable-rate orchard sprayer based on a laser-scanning sensor. *Int. J. Agric. Biol. Eng.* **2019**, *12*, 51–57. [[CrossRef](#)]

37. Li, L.; He, X.; Song, J.; Liu, Y.; Zeng, A.; Liu, Y.; Liu, C.; Liu, Z. Design and experiment of variable rate orchard sprayer based on laser scanning sensor. *Int. J. Agric. Biol. Eng.* **2018**, *11*, 101–108. [[CrossRef](#)]
38. Xiao, K.; Ma, Y.; Gao, G. An intelligent precision orchard pesticide spray technique based on the depth-of-field extraction algorithm. *Comput. Electron. Agric.* **2017**, *133*, 30–36. [[CrossRef](#)]
39. Zeng, L.; Feng, J.; He, L. Semantic segmentation of sparse 3D point cloud based on geometrical features for trellis-structured apple orchard. *Biosyst. Eng.* **2020**, *196*, 46–55. [[CrossRef](#)]
40. Yandún, N.; Salvo, D.; Prieto, P.; Torres-Torriti, M.; Auat, F. LiDAR and thermal images fusion for ground-based 3D characterisation of fruit trees. *Biosyst. Eng.* **2016**, *151*, 479–494. [[CrossRef](#)]

Disclaimer/Publisher’s Note: The statements, opinions and data contained in all publications are solely those of the individual author(s) and contributor(s) and not of MDPI and/or the editor(s). MDPI and/or the editor(s) disclaim responsibility for any injury to people or property resulting from any ideas, methods, instructions or products referred to in the content.